



Mechanical behavior and physicochemical modifications in lignosulfonate-treated fique (*Furcraea Andina*) fibers

Beatriz Dantas Lourenço da SILVA¹, Paula Lage AGRIZE¹, Betina Carvalho VEIGA¹, Lucio Fabio Cassiano NASCIMENTO², Camila Aparecida Abelha ROCHA¹ and Fábio de Oliveira BRAGA^{1,*}

¹ Universidade Federal Fluminense (UFF), Department of Civil Engineering, Rua Passo da Pátria 156, Bloco D, 4º andar, Niterói, Rio de Janeiro, 24210-240, Brazil

² Instituto Militar de Engenharia (IME), Department of Materials Science, Praça General Tibúrcio 80, Urca, Rio de Janeiro, 22290-270, Brazil

*Corresponding author e-mail: fabiobraga@id.uff.br

Received date:

1 November 2022

Revised date

1 February 2023

Accepted date:

19 February 2023

Keywords:

Natural lignocellulosic fiber;
Surface treatment;
Physical properties;
Mechanical properties;
Microstructure

Abstract

One of the most frequent problems in biocomposites is the physical/chemical incompatibility between natural lignocellulosic fibers (NLF) and the matrix. Physical and/or chemical treatments are the most common approach to improve interface properties. Seeking for environmentally friendly treatments, lignosulfonates (LSs) have been considered for surface modification of NLF due to their amphiphilic properties. Thus, the objective of the present work is to evaluate the influence of sodium LS (SLS) treatment protocols in the properties and mechanical behavior of fique (*Furcraea Andina*) fibers. X-ray diffraction (XRD), Thermogravimetric (TGA) and spectroscopic (FTIR) analyzes were performed, as well as optical microscopy, scanning electron microscopy (SEM), fiber-diameter measurements and tensile tests. The results showed efficient surface cleaning from extractives and absorption of saline and aromatic components from SLS. Partial removal of lignin and hemicellulose was observed as well, manifested by an increasing in fiber crystallinity, decreasing in the intensity of the characteristic bands of C=O (acetyl and ester) and p-hydroxy-phenyl, and displacement in the temperature of cellulose pyrolysis to lower temperatures. These phenomena were stronger in the fibers with longer exposures to SLS. The SLS treatment protocols produce a narrower strength distribution, improving the reliability of the fibers relative to its mechanical behavior.

1. Introduction

Over the last 30 years, utilization of natural lignocellulosic fibers (NLF) has been rapidly increasing, due to their interesting properties such as high strength and stiffness, low density and cost, as well wide availability from natural sources [1-4]. These fibers have been left aside due to the advent of the synthetic fibers in the middle part of the twentieth century. However, environmental concerns brought NLF again to attention of scientific community [4-6].

One of the most promising applications for NLF is composite reinforcement. There are several successful cases in engineering and research [1-11]. NLF have shown good results as reinforcement of polymers [1-7], Portland cement and other mineral-based matrices [8-11]. They are known to increase tensile, flexure and impact strength of these materials, as well as maximum deformation, either extension or deflection [1-11].

Biocomposites reinforced with NLF are considered more sustainable than synthetic fiber composites, since their production and processing involve lower energy consumption and net-zero carbon emission in the fiber life cycle [12]. This alternative drives research in the area, seeking to improve the properties of the produced materials.

Fique fibers (*Furcraea Andina*) are promising for composites application due to their long length and good properties. Colombia native, but also produced in Ecuador, Costa Rica, Antilles and Brazil [13], fique fibers are considered resistant, rigid and with a smooth surface [13-17]. Gañán and Mondragon [13] reported tensile strength of 237 ± 51 MPa, modulus of elasticity of 8.01 ± 1.47 GPa and total elongation of $6.02 \pm 0.69\%$ [13,14]. According to Bastidas [14], the dry mass of the raw fique fibers is composed of cellulose (42.1 ± 0.6 wt%), hemicellulose (13 ± 0.4 wt%), lignin (18.2 ± 0.8 wt%), extractives (15.3 ± 0.3 wt%) and ashes (1.1 ± 0.2 wt%). They also reported [14] that the thermal degradation of the fibers occurs around 360°C. Due to their good properties, several researchers are currently investigating the properties of fique fibers for composite reinforcement [18].

One of the most frequent problems to be faced for biocomposites is the chemical incompatibility between fiber and matrix. Surface physicochemical treatments are the most common approach to improve fiber-matrix interface properties [19-22].

In search of an environmentally friendly treatment, lignosulfonates (LSs) have been considered and applied for surface modification of NLF with interesting results [23-25]. LSs are chemicals produced in the sulfite pulping process of wood, from the breakage of the lignin

polymer chain [26]. According to Ruwoldt [26], there are several types of lignosulfonates, such as sodium, magnesium, calcium, and ammonium. LSs are characterized by their anionic, surfactant, binding, wetting and plasticizing behavior. When wet, LSs develop adhesiveness and agglomeration power. Still according to Ruwoldt [26], LSs have amphiphilic properties, having both hydrophilic and hydrophobic constituents in its molecular structure, and thus can adsorb to several surfaces and interfaces. Anionic groups such as sulfonate and carboxylic ensure water solubility, while less polar groups such as aromatic and aliphatic chains facilitate interaction with organic surfaces and interfaces [26].

The use of LSs as NLF surface treatment agents has been attempted with good results for modification of natural fibers such as sisal and wool [23-25]. Jose *et al.* [23] studied the modification of wool fabric with sodium LS (SLS) to improve the interfacial adhesion of natural rubber latex in the wool/rubber composites. They found out that the SLS acted as a cementing material between the wool fiber and latex, resulting in improved composite properties, such as better elongation and retention of tensile strength after UV ageing [23]. Oliveira *et al.* [24] studied the modification of sisal fibers with SLS to improve the properties of phenolic-matrix composites. The results showed greater impact strength of the composites reinforced with SLS-modified sisal fibers. Gualberto *et al.* [25] studied the treatment of sisal fibers with SLS to improve the properties of cement-matrix composites. The resulting composites showed better tenacity and better fiber-matrix adhesion. However, the action of the LSs in lignocellulosic fibers needs to be further studied, and currently there is no investigation that evaluates the influence of LSs in the structure and properties of fique (*Furcraea Andina*) fibers. Therefore, the objective of the present work is to evaluate mechanical, physical, and chemical changes in the fique fibers when subjected to several treatment protocols using SLS. Thus, the present work evaluates for the first time the physico-chemical modifications of the fique fibers subjected to specific SLS treatment protocols and might be important to understand further studies on fiber-matrix adhesion in composites.

2. Experimental

2.1 Materials

2.1.1 Fique fibers

For the development of this work, fique fibers (*Furcraea Andina*) (Figure 1) were acquired from local producers in Colombia. The fibers were manually cleaned with a nylon hairbrush, to remove some dry wax and to individualize (separate) them. The fibers were then cut to the lengths specified to each test.

2.1.2 Sodium lignosulfonate (SLS)

Sodium lignosulfonate (SLS) was used as modification agent of the fibers. The SLS powder was provided by Lignotech Brasil (Brazil), from the Borregaard Lignotech group, type 1259 Ultrazine NA (CAS No. 8061-51-6). According to the manufacturer, Ultrazine NA is based on highly refined and modified sodium lignosulfonate derived from spruce wood and sulfite liquor. It was provided as a brown water-soluble powder. Table 1 show some basic specifications of the chemical.



Figure 1. General aspect of the fique fibers.

Table 1. Basic Specifications of the Borregaard Ultrazine NA.

Sales specifications	
pH (10% solution)	8.7 ± 0.8
Insolubles (%w/w)	Max. 0.1
Sodium %	7
Calcium %	Max. 0.1
Reducing sugars %	1
Chloride %	Max. 0.10
Alkali %	Max. 12%

Table 2. Specimen designation.

Treatment protocol	Specimen designation
1h immersion in water at 70°C	Raw fique
1h immersion in 5 wt% SLS solution at 70°C	FL-70-1h
24h immersion in 5 wt% SLS solution at 25°C	FL-24h
1h immersion in 5 wt% SLS solution at 25°C in the ultrasonic bath	FL-1h-US

2.2 Methods

2.2.1 Fiber processing

The dry and cut fibers were separated into 4 groups, 3 for the SLS treatment protocols and 1 for the control group. The fibers from the control group were immersed in 70°C deionized water for 1 h, and then dried in the oven at 104 ± 2°C until constant mass. The fibers from this group were designated as Raw Fique (Table 2). The SLS treatment protocols were carried out by immersing the fibers in a 5 wt% SLS solution in deionized water. These treatment protocols were previously employed to other natural fibers by other researchers [24,25], with good results.

The first SLS treatment was very similar to the control group, however, the fibers were immersed in the 5 wt% SLS solution (at 70°C for 1 h) instead of pure deionized water. The fibers from this group were designated as FL-70-1h (Table 2). In the second SLS treatment, the fibers were immersed in the 5 wt% SLS solution for 24 h at room temperature (25°C). The fibers from this group were designated as FL-24h (Table 2). In the third treatment, the fibers were immersed in the 5 wt% SLS solution for 1h subjected to ultrasonic irradiation (40 kHz), in a laboratory ultrasonic bath, model SoniClean 2PS (Sanders). The fibers from this group were designated as FL-1h-US (Table 2). After each treatment, the fibers were dried in an oven until reaching constant mass.

The objective of using ultrasonic energy was to increase the surface free energy of the fibers, to make the surface more active and receptive to the SLS molecules. The ultrasonic vibration is known to cause cavitation, a physicochemical phenomenon of formation and outbreak of bubbles [24].

2.2.2 Optical microscopy and diameter measuring

The optical micrographs of the fibers were obtained in a model LAB-60T Laborana stereomicroscope. The diameter measuring of the fibers was performed in a model BX3M Olympus optical microscope. The fibers were positioned one by one, stretched, fixed on a cardboard fillet, and observed at 100x magnification. Thirty-five fibers from each treatment were analyzed. The images were captured by a camera attached to the microscope, and the diameters were measured at three different points along the length, using LCmicro software. The data was treated using Analysis of Variance (ANOVA) to evaluate the statistical significance of any diameter variation.

2.2.3 Scanning Electron Microscopy (SEM)

The SEM analyzes were performed in a model Quanta FEG 250 FEI scanning electron microscope, to evaluate the modifications in the surface of the fibers. Secondary electrons contrast was used to observe the surface morphology, as well as Energy-dispersive X-ray spectroscopy (EDS) analysis to correlate the images to their chemical composition.

2.2.4 X-Ray Diffraction (XRD)

The X-ray diffraction analyzes were performed to evaluate the changes in the crystal structure and degree of crystallinity of the fibers, resulting from the SLS treatments. A model D8 Advance Polycrystal Bruker diffractometer was used. Intensity measurements were performed in the 2θ range between 10° and 70° , with a 0.05° step and $2^\circ \cdot \text{min}^{-1}$ scanning velocity. As sample preparation, the fibers were cut with scissors to lengths of less than 1 mm. To estimate the Crystallinity Index (X_c) of the raw and treated fique fibers, the diffraction patterns were processed using Origin 8 software, to obtain data on the peaks of cellulose and amorphous phases. The crystallinity index (X_c) is calculated from Equation (1) [27,28]:

$$X_c = \frac{I_{002} - I_{am}}{I_{002}} \cdot 100\% \quad (1)$$

Where: X_c is the fiber crystallinity index; I_{002} is the maximum intensity (in arbitrary units) of the (002) lattice diffraction peak (2θ around 22°); I_{am} is the height of the minimum between the (002) and the (101) peaks (minimum at 2θ around 18.5°).

2.2.5 Fourier transform infrared spectroscopy (FTIR)

The fibers were analyzed by means of Fourier transform infrared spectroscopy (FTIR), in the Attenuated Total Reflection (ATR) mode, to evaluate chemical changes resulting from the SLS treatment protocols. The spectra were obtained using a model Spectrum 100 Perkin Elmer infrared spectrometer, in the range of 4000 cm^{-1} to 650 cm^{-1} . The spectra were analyzed following ASTM D2224 standard [29].

2.2.6 Thermogravimetric analysis (TGA)

The thermogravimetric analysis (TGA) was performed to evaluate the thermal stability of the fibers before and after the SLS treatments. The analyzes were performed in a model DTG-60 Shimadzu equipment, from ambient temperature (21°C) to 500°C , at a heating rate of $10^\circ\text{C} \cdot \text{min}^{-1}$, in a nitrogen atmosphere. The spectra were analyzed following ASTM E2550 standard [30].

2.2.7 Tensile tests

Tensile tests of the raw and treated fibers were carried out following the procedures of the ASTM C1557 standard [31], using a model Tytron 250 MTS testing machine. 12 samples were tested for each treatment, with a test speed of $0.3 \text{ mm} \cdot \text{min}^{-1}$, a 5 kN load cell and a working length of 40 mm. The experimental setup for the tensile test is shown at Figure 2.

Due to specimen variability, the test results were statistically treated by fitting the data to a 2-parameter Weibull distribution [32], characterized by a shape parameter (β) and a scale parameter (θ), as well as the adjustment R^2 . The Weibull cumulative distribution function is given by Equation (2):

$$F(x) = 1 - e^{-\left(\frac{x}{\theta}\right)^\beta} \quad (2)$$

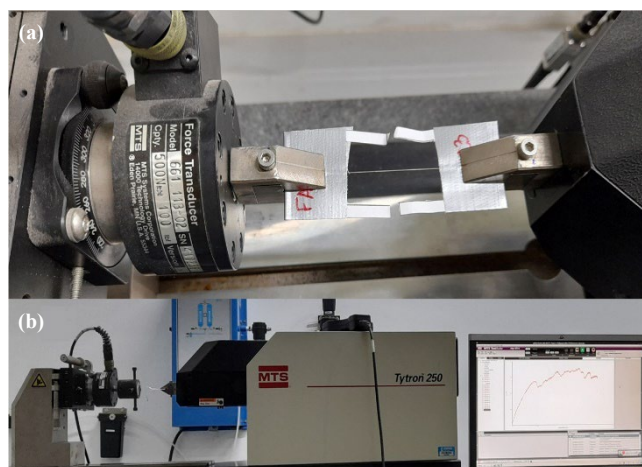


Figure 2. Experimental setup for the tensile test of the fibers.

3. Results and discussion

3.1 Optical microscopy and diameter measuring

Figure 3 shows the optical micrographs of the untreated (Figure 3(a)) and treated fibers (Figure 3(b-d)). The fibers are composed of microfibrils oriented along the fiber axis, with specific features depending on the treatment. The untreated fiber (Raw fique, Figure 3(a)) presents dark marks on the surface, which are probably related to impurities, such as waxes and other extractives. These dark marks could not be observed on the treated fibers (Figure 3(b-d), which show cleaner surfaces, especially the FL-70-1h specimen. Figure 3(b-d) show, also, bright marks spread through the surface, which are probably SLS crystals.

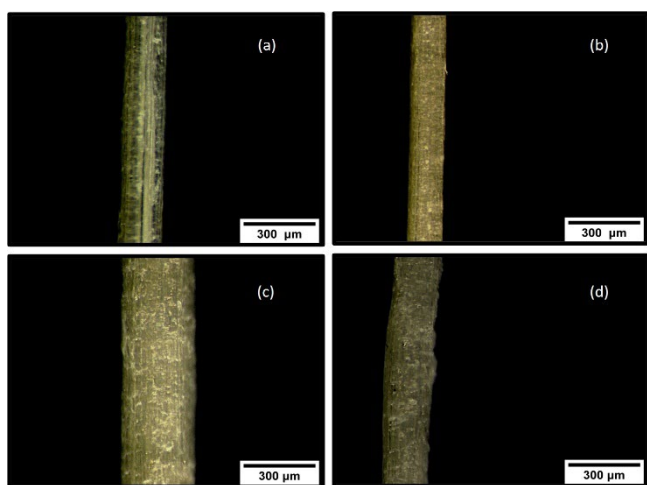


Figure 3. Optical micrographs of the fique fibers, captured by the LAB-60T Laborana stereomicroscope: (a) Raw fique; (b) FL-70-1h; (c) FL-24h; (d) FL-1h-US.

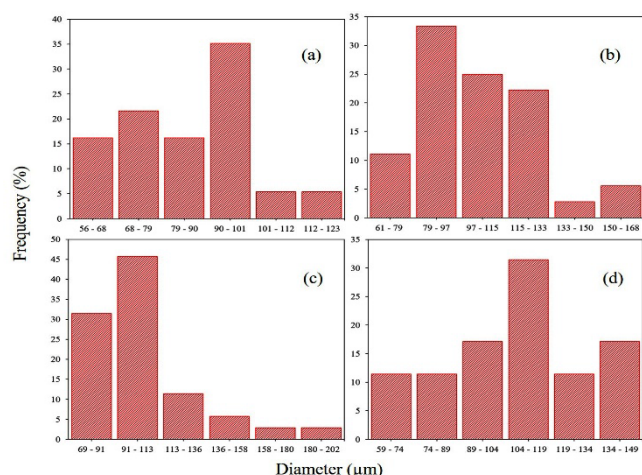


Figure 4. Diameter distributions for the fibers: (a) Raw fique; (b) FL-70-1h; (c) FL-24h; (d) FL-1h-US.

Table 3. Fiber diameter (d) data.

Specimen	d_{max} (μm)	d_{min} (μm)	d_m (μm)	σ (μm)
Raw fique	123	56	84	15
FL-70-1h	168	61	103	24
FL-24h	202	69	105	28
FL-1h-US	149	59	106	24

Figure 4 shows histograms containing the diameter distributions for the fibers. The most frequent diameters are included in the interval from ~ 80 and $120 \mu\text{m}$. Table 3 shows the minimum (d_{min}), maximum (d_{max}), and average (d_m) diameter values, together with the standard deviation (σ) of the distributions. Diameters greater than $125 \mu\text{m}$ were only found among the treated fibers, and minimum values were slightly greater than the observed values for the Raw fique fibers. However, the Analysis of Variance (ANOVA) indicated that the average values should be considered statistically similar (p-value 0.976888), considering significance level of 5%. Differences in the average diameters were not expected, since the result of the treatment protocols would be to provide a thin layer of SLS and crystallization products on the fibers surface.

3.2 Scanning Electron Microscopy (SEM)

Figure 5 to Figure 8 show the SEM micrographs of the fibers. Figure 5 confirms that Raw fique fibers present extractives on the surface, which might be removed by the treatment protocols. The EDS analysis showed presence of carbon (C), oxygen (O) and calcium (Ca). As widely known, C and O are the basic elements of the lignocellulosic structure. About Ca, Ovalle-Serrano [16] reported that the element is useful to the plant to structurally preserve the cell wall. Figure 6 shows that the FL-70-1h treatment was able to remove these impurities. Besides C, O and Ca, traces of sodium (Na) were identified by the EDS analysis, indicating absorption of SLS components.

Figure 7 shows that the FL-24h treatment protocol was also able to remove the extractives, however, intense precipitation of SLS crystallization products was observed. As for FL-70-1h treatment, EDS analysis of the FL-24h surface also shows C, O, Ca and traces of Na.

Figure 8 shows that FL-1h-US treatment is also efficient to remove the impurities, and, unlike FL-70-1h and FL-24h, no traces of Na were identified, so only C, O and Ca were found.

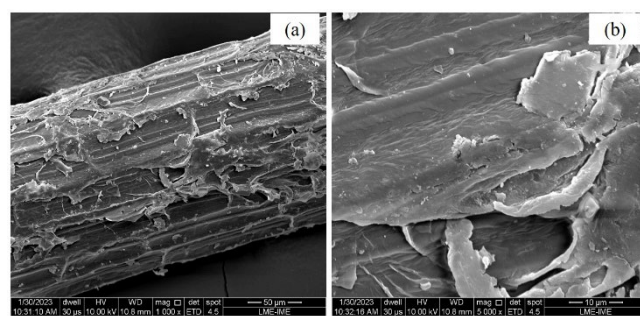


Figure 5. SEM micrographs of the Raw fique fibers: (a) 1,000x, and (b) 5,000x.

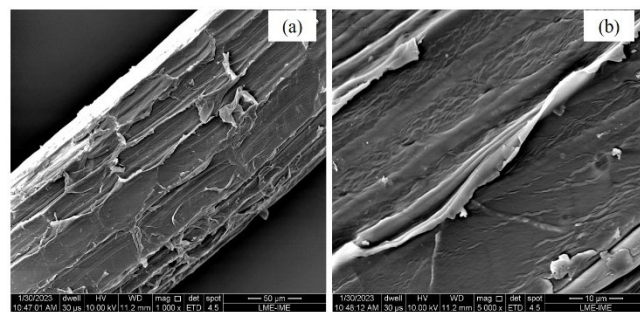


Figure 6. SEM micrographs of the FL-70-1h: (a) 1,000x, and (b) 5,000x.

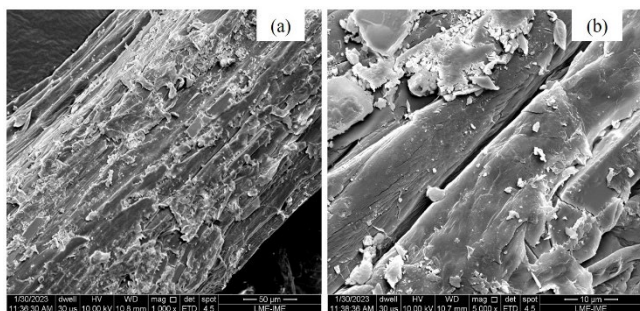


Figure 7. SEM micrographs of the FL-24h: (a) 1,000x, and (b) 5,000x.

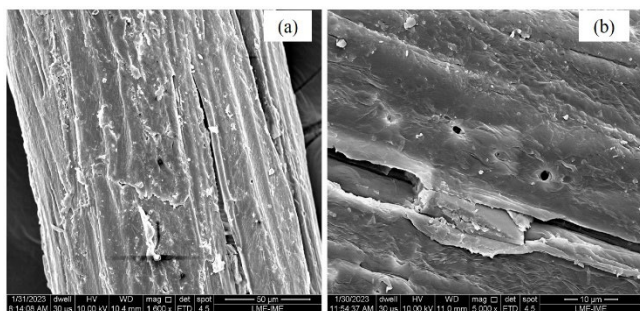


Figure 8. SEM micrographs of the FL-1h-US: (a) 1,600x, and (b) 5,000x.

3.3 X-Ray diffraction (XRD)

Figure 9 shows the diffraction patterns for fique fibers. Typical peaks for the native cellulose (ICDD database, PDF 03-0289) are present, as summarized in Table 4 [16,33]. The small peaks at 30.6° and 38.7° (Figure 9) were not included in Table 4, since they were not reported in the aforementioned references [16,33], however, they were also identified as native cellulose, according to the PDF 03-0289 file.

The crystallinity index (X_c) has been calculated from the diffraction patterns (Figure 9) and the data are presented in Table 5. The obtained X_c values (Table 5) are coherent with literature values [16] and are consistent with the common cellulose content around 30% to 50% [14, 16]. Since cellulose is considered the only relevant crystalline compound in the NLFs, X_c should follow the values of cellulose content. Ovalle-Serrano [16], for example, obtained $X_c = 63\%$ for raw fique fibers, $X_c = 57\%$ for fique tow and $X_c = 35\%$ for fique pulp. These values show correlation with the cellulose content of those specimens, $52.9 \pm 2.1\%$, $52.3 \pm 3.1\%$ and $31.5 \pm 1.1\%$, respectively. This is an indication that increasing cellulose content due to lignin and hemicellulose dissolution would explain the variation of X_c . In the present work, the SLS increased the crystallinity of the fique fibers for all treatment protocols. Also, longer treatment times, such as in FL-24h specimen, could favor the phenomenon of lignin, hemicellulose and other extractives dissolution, increasing the resulting crystallinity.

3.4 Fourier-transform infrared spectroscopy (FTIR)

Figure 10 shows the FTIR spectra for the several specimens. Figure 10 shows that typical lignocellulosic groups are present in all specimens. 3341 cm^{-1} absorption band is attributed to OH stretching due to phenolic and open alcoholic groups. 2923 cm^{-1} band is attributed

to C-H stretching due to methyl and other alkyl groups. 1733 cm^{-1} band is attributed to C=O stretching vibration in acetyl and ester groups in lignin, hemicellulose and pectin [22]. 1604 cm^{-1} is attributed to C=C vibration due to aromatic rings in lignin [22,34]. 1026 cm^{-1} band is attributed to C-O stretching and C-H vibration, both present in the lignocellulosic compounds (cellulose, hemicellulose and lignin). 895 cm^{-1} band is associated with the cellulosic β -glycosidic linkages [16,22]. 663 cm^{-1} is attributed to S-O stretching in sulfonic groups, which, according to Jose *et al.* [23] results from the response of sodium sulfite with the secondary hydroxyl of the aliphatic side chain of lignin.

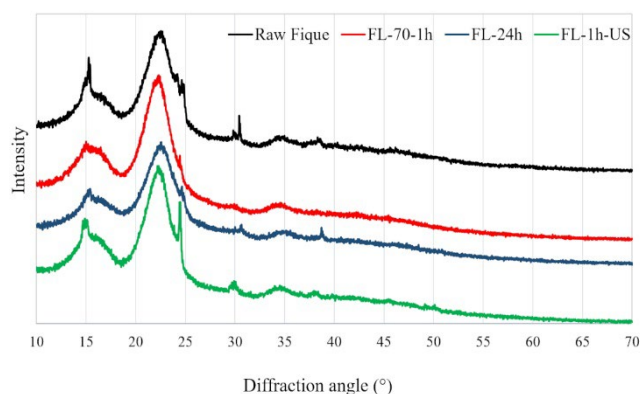


Figure 9. X-ray diffraction patterns for the raw and treated fibers.

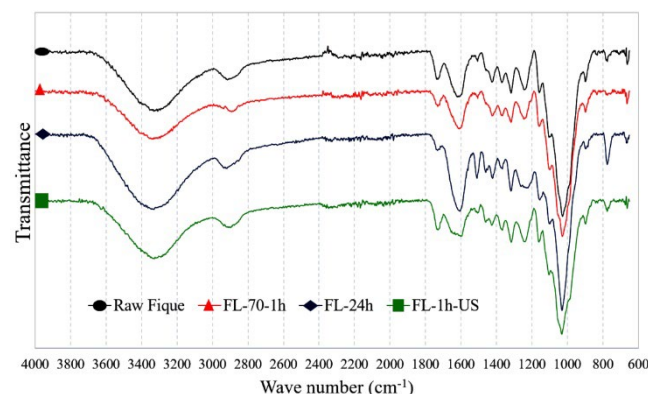


Figure 10. FTIR spectra for the raw and treated fibers.

Table 4. Peak information from the XRD spectra of the raw and treated fique fibers.

Peak position (degrees)	Structure	Crystalline plane
15.0	Cellulose I	(110) [16,33]
16.5	Cellulose I	(1 $\bar{1}$ 0) [33]
22.5	Cellulose I	(200) [16,33]
35.0	Cellulose I	(004) [16,33]

Table 5. Peak intensity data and calculated crystallinity index (X_c).

Specimen	I_{002}	I_{am}	X_c (%)
Raw fique	9453	6744	28.7
FL-70-1h	7266	4053	44.2
FL-24h	4362	2074	52.4
FL-1h-US	8494	5363	36.9

Analyzing the spectra (Figure 10), it can be noticed that the FL-70-1h spectrum is the most similar to the untreated fiber (Raw fiqu), which indicates that the treatment with SLS for 1h at 70°C had little effect in the chemistry of the fiqu fibers. Apart from that, the main differences between the spectra are detailed below: (a) 1733 cm^{-1} (C=O) band is less intense for FL-24h and FL-70-1h spectra, indicating a decrease of C=O related groups such as acetyl and ester groups. This has been observed by Gañan and Mondragon [13] for the mercerization process of a lignocellulosic fiber that resulted in removal of some lignin (and hemicellulose); (b) 831 cm^{-1} band is absent in the FL-24h spectrum, which is an indication of breaking of the p-hydroxy-phenyl groups in lignin, also compatible to mercerization process in alkaline medium. It is important to mention that SLS solutions are alkaline, and their pH is around 8.7, according to the supplier's datasheet; (c) The band in 775 cm^{-1} has a higher intensity in the FL-24h spectrum, which, together with the 895 cm^{-1} band shoulder, indicates the absorption of saline compounds from SLS by the fibers [35,36]. The presence of the 1230 band (S=O) corroborates this information, although this band might be overlapped with C-C and C-O group absorptions [33-36]; (d) Bands at 1604 cm^{-1} and 1508 cm^{-1} (C=C) are more intense for FL-24h, and a little less for FL-1h-US. These are related to vibration of the aromatic skeleton of lignin [13,37]. These absorptions together with the 1260 cm^{-1} (guaiacyl) in FL-24h, suggests that, although p-hydroxy-phenyl groups in lignin are decreasing (partial degradation of lignin in the fiber), other groups such as guaiacyl are increasing, probably due to introduction of lignin-related groups from SLS.

3.5 Thermogravimetric analysis (TGA)

Figure 11 shows the thermogravimetric (TG) curves for the raw and treated fibers. All specimens presented three specific features: (a) a small mass drop ($\sim 10\%$) below 100°C due to vaporization of moisture; (b) an intense weight loss (50% to 70%) in the 250°C to 350°C temperature range; (c) a smooth and continuous mass loss over 350°C. According to several authors [13,14,16,24], (b) is due to thermal depolymerization of hemicellulose ($\sim 250^\circ\text{C}$) and pyrolysis of cellulose ($\sim 350^\circ\text{C}$). Figure 12 shows these two processes for the Raw fiqu, by the separation of the two reaction minima in the DTG curve.

The weight losses in (b) are consistent to the lignocellulosic composition observed by Bastidas [14]. According to the authors [14], cellulose and hemicellulose contents in the fiqu fibers were $42.1 \pm 0.6 \text{ wt}\%$ and $13 \pm 0.4 \text{ wt}\%$, respectively, which would totalize a weight loss around 55%. This is consistent to the information on Figure 11, which shows a 50% to 70% weight loss. Partial degradation of lignin could occur simultaneously to hemicellulose and cellulose, which would complete the degradation process.

The disappearing of one reaction minimum on the DTG curves (Figure 12) for the treated specimens (FL-70-1h, FL-24h and FL-1h-US)

is an important feature. This could be explained by the suppression of the hemicellulose degradation at 300°C, due to the removal of hemicellulose by the SLS treatments. The thermal event at 300°C is probably due to cellulose degradation, which has been displaced to lower temperatures, since cellulose became more susceptible to thermal degradation, as observed by Oliveira *et al.* [24]. The variation on the residual mass is also consistent with the phenomenon of removal of hemicellulose/lignin. FL-24h and FL-1h-US were the specimens of higher residual mass, indicating that a higher content of extractives has been removed during the treatments.

The reactions at 400°C and 450°C are only observed for the treated fibers and could be related to decomposition of aromatic rings of the SLS [24].

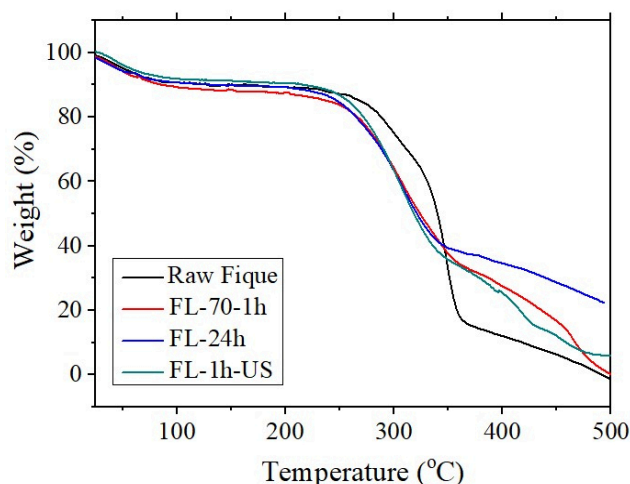


Figure 11. TG curves for the raw and treated fibers.

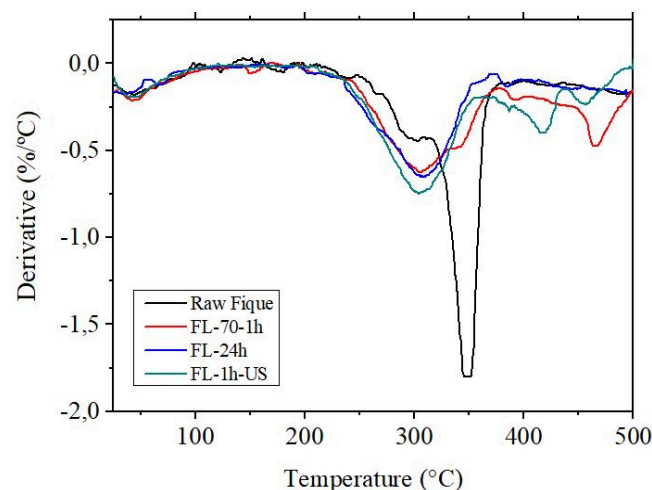


Figure 12. DTG curves for the raw and treated fibers.

Table 6. Tensile test data obtained from the stress-strain curves.

Specimen	Strength			Maximum strain		
	β (MPa)	θ (MPa)	R^2	β (%)	θ (%)	R^2
Raw fiqu	1.31	283.44	0.92	2.09	10.33	0.74
FL-70-1h	1.46	167.51	0.93	2.13	14.07	0.90
FL-24h	2.38	159.24	0.94	2.57	14.20	0.98
FL-1h-US	2.33	147.46	0.94	1.95	11.58	0.90

3.6 Tensile tests

Figure 13 shows the tensile stress-strain curves for the fibers. The curves in Figure 13 show typical elastic stress-strain behavior until fracture and a broad variability of values for strength and maximum strain, attributed to diameter variation and other known heterogeneities in the fibers [38]. Table 6 show the Weibull statistical parameters applied to strength and maximum strain. The scale parameter (θ) represents the approximate center of the distribution, the value under which 63.2% of the fibers will fail, while the shape

parameter (β) represents the variability of the data. The larger β , the narrower is the distribution. Figure 14 shows the distribution plots obtained from the parameters in Table 6. The results show that all treatments, especially FL-24h and FL-1h-US, produces a narrower strength distribution, improving the reliability of the fibers relative to its mechanical behavior. This is probably due to the partial removal of hemicellulose/lignin, which decreases the number of critical defects on the fibers. On the other hand, the treatments do not seem to influence the maximum deformation.

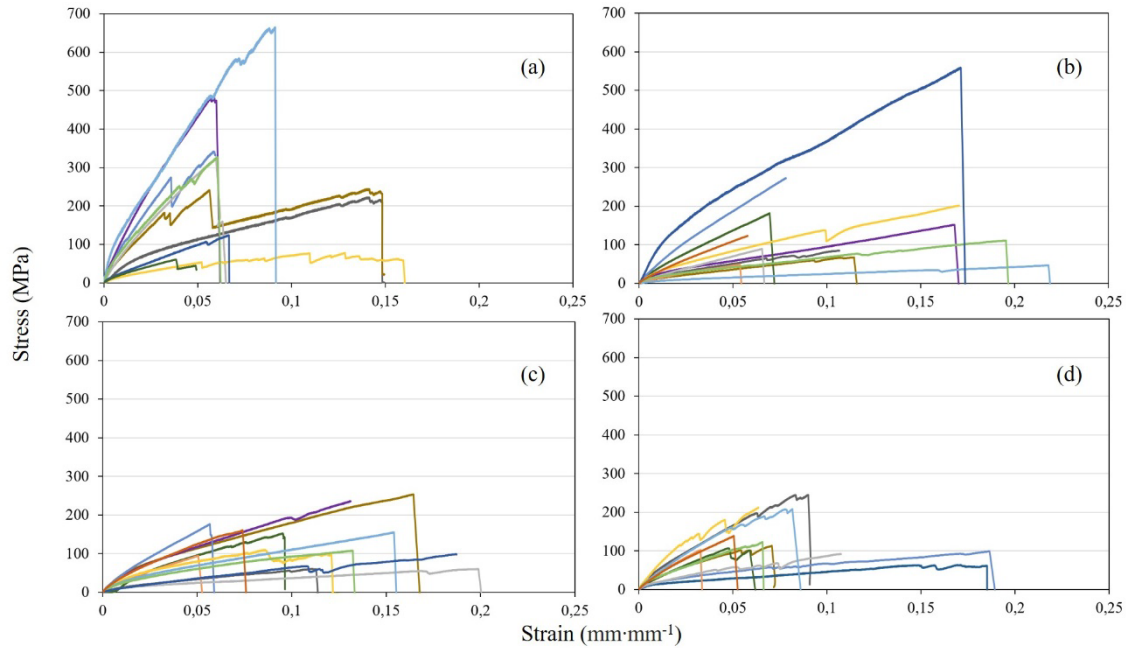


Figure 13. Tensile stress-strain curves for the fibers: (a) raw fique; (b) FL-70-1h; (c) FL-24h; (d) FL-1h-US.

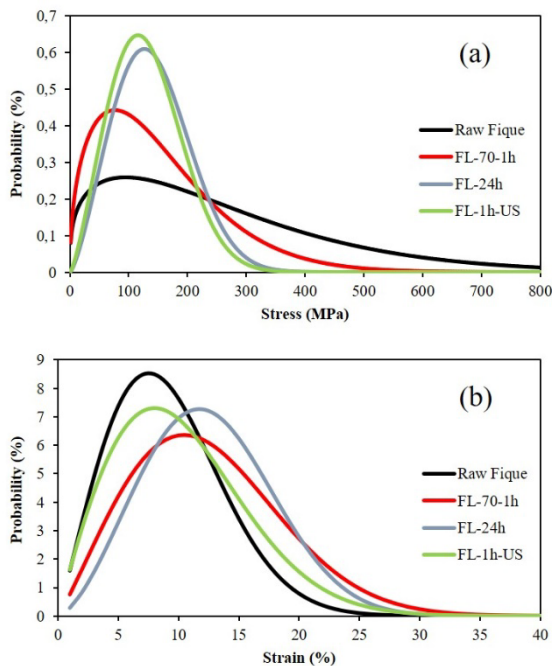


Figure 14. Weibull density of probability function for (a) strength; (b) maximum extension.

4. Conclusions

In the present work, several treatment protocols using sodium liginosulfonate (SLS) were applied to fique (*Furcraea Andina*) fibers, to evaluate the mechanical, physical, and chemical changes. The treatment protocols were: (1) Raw fique (control group): 1-h immersion in deionized water at 70°C; (2) FL-70-1h: 1-h immersion in 5 wt% SLS solution at 70°C; (3) FL-24h: 24-h immersion in 5 wt% SLS solution at room temperature (25°C); (4) FL-1h-US: 1-h immersion in 5 wt% SLS solution in conjunction with ultrasonic irradiation (40 kHz). The main conclusions are presented below:

- All evaluated SLS treatments protocols were efficient in cleaning the fiber surface from extractives, however, caused deposition of SLS products over the fiber surface, especially the FL-24h, which produced intense deposition of crystallization products.
- SLS treatment protocols did not significantly change the fibers average diameter. The most frequent observed diameters were included in the range from $\sim 80 \mu\text{m}$ and $120 \mu\text{m}$.
- SLS treatment protocols increased the crystallinity of fique fibers due to lignin, hemicellulose, and other extractives dissolution. The treatment protocol with higher influence on the fiber crystallinity was the FL-24h.

- FL-70-1h treatment did not significantly affect the fiber chemistry. On the other hand, the treatment with higher influence in the fiber chemistry was the FL-24h, which caused a decreasing in the amount of C=O related groups (acetyl and ester groups) and breaking of the p-hydroxy-phenyl groups in lignin, due to lignin (and hemicellulose) removal. Absorption of saline and aromatic compounds from SLS was observed in all treated specimens.

- Cellulose pyrolysis has been displaced to lower temperatures for all treated specimens, indicating that cellulose became more susceptible to thermal degradation. Thermal reactions around 400°C and 450°C were observed for the treated fibers, probably due to decomposition of aromatic rings of the deposited SLS.

- The tensile behavior of the untreated and treated fibers was characterized by typical elastic stress-strain behavior until fracture and a broad variability of values for strength and maximum strain, due to diameter variation and other heterogeneities in the fibers. The SLS treatment protocols produce a narrower strength distribution, improving the reliability of the fibers relative to its mechanical behavior, probably due to the (partial) removal of hemicellulose/lignin, which decreases the number of critical defects.

Acknowledgements

The authors of the present work would like to acknowledge: FAPERJ for funding the project in the Basic Research Aid (APQ1) Program, process 211.544/2021; UFF/Brazil Research Funding Program (FOPESQ 2021), for funding the project; PPGCM/IME/Brazil for the donation of the fique fibers, as well as enabling the diameter measuring, SEM and FTIR analyzes; NUMATS/COPPE/UFRJ/Brazil for performing the tensile tests; LDRX/IF/UFF/Brazil for performing the XRD tests; RECAT/UFF/Brazil for performing the thermogravimetric analyzes; Lignotech Brasil, for the donation of the lignosulfonate.

References

- [1] T. Vaisanen, O. Das, and L. Tomppo, "A review on new bio-based constituents for natural fiber-polymer composites," *Journal of Cleaner Production*, vol. 149, pp. 582-596, 2017.
- [2] A. Lotfi, H. Li, D. V. Dao, and G. Prusty, "Natural fiber-reinforced composites: A review on material, manufacturing, and machinability," *Journal of Thermoplastic Composite Materials*, vol. 34, no. 2, pp. 238-284, 2019.
- [3] M. Zwawi, "A Review on natural fiber bio-composites, surface modifications and applications," *Molecules*, vol. 26, pp. 404-431, 2021.
- [4] S. K. Ramamoorthy, M. Skrifvars, and A. Persson, "A review of natural fibers used in biocomposites: plant, animal and regenerated cellulose fibers," *Polymer Reviews*, vol. 55, pp. 107-162, 2015.
- [5] O. Faruk, A. K. Bledzki, H-S. Fink, and M. Sain, "Progress report on natural fiber reinforced composites," *Macromolecular Materials and Engineering*, vol. 299, pp. 9-26, 2014.
- [6] O. Faruk, A. K. Bledzki, H-S. Fink, and M. Sain, "Bio-composites reinforced with natural fibers: 2000-2010," *Progress in Polymer Science*, vol. 37, pp.1552-1596, 2012.
- [7] R. S. Castoldi, L. M. S. Souza, and F. A. Silva, "Comparative study on the mechanical behavior and durability of polypropylene and sisal fiber reinforced concretes," *Construction and Building Materials*, vol. 211, pp. 617-628, 2019.
- [8] F. Pacheco-Torgal, and S. Jalali, "Cementitious building materials reinforced with vegetal fibers: A review," *Construction and Building Materials*, vol. 25, pp. 575-581, 2011.
- [9] R. P. Fonseca, J. C. Rocha, and M. Cheriah, "Mechanical properties of mortars reinforced with amazon rainforest natural fibers", *Materials*, vol. 14, pp. 155-173, 2021.
- [10] P. F. P. Ferraz, R. F. Mendes, D. B. Marin, J. L. Paes, D. Cecchin, and M. Barbari, "Agricultural residues of lignocellulosic materials in cement composites," *Applied Sciences*, vol. 10, pp. 8019-8036, 2020.
- [11] A. Jesudass, V. Gayathri, R. Geethan, M. Gobirajan, and M. Venkatesh, "Earthen blocks with natural fibres - A review," *Materials Today: Proceedings*, vol. 45, no. 7, pp. 6979-6986, 2021.
- [12] S. V. Joshi, L. T. Drzal, A. K. Mohanty, and S. Arora, "Are natural fiber composites environmentally superior to glass fiber reinforced composites?," *Composites Part A: Applied Science and Manufacturing*, vol. 35, pp. 371-376, 2004.
- [13] P. Gañán, and I. Mondragon, "Surface modification of fique fibers: Effects of their physico-mechanical properties," *Polymer Composites*, vol. 23, no. 3, pp: 383-394, 2002.
- [14] K. G. Bastidas, M. F. R. Pereira, C. A. Sierra, and H. R. Zea, "Study and characterization of the lignocellulosic Fique (*Furcraea Andina* spp.) fiber," *Cellulose*, vol. 29, pp. 2187-2198, 2022.
- [15] M. C. A. Teles, G. R. Altoé, P. A. Netto, H. A. Colorado, F. M. Margem, and S. N. Monteiro, "Fique fiber tensile elastic modulus dependence with diameter using the Weibull statistical analysis," *Materials Research*, vol. 18 (Suppl. 2), pp. 193-199, 2015.
- [16] A. S. Ovalle-Serrano, C. Blanco-Tirado, and M. Y. Combariza, "Exploring the composition of raw and delignified Colombian fique fibers, tow and pulp," *Cellulose*, vol. 25, pp. 151-165, 2018.
- [17] S. N. Monteiro, F. S. Assis, C. L. Ferreira, N. T. Simonassi, R. P. Weber, M. S. Oliveira, H. A. Colorado, and A. C. Pereira, "Fique fabric: A promising reinforcement for Polymer composites," *Polymers*, vol. 10, pp. 246-255, 2018.
- [18] S. Gómez-Suarez, and E. Córdoba-Tuta, "Composite materials reinforced with fique fibers – A review," *Revista UIS Ingenierías*, vol. 21, no. 1, pp. 163-178, 2022.
- [19] D. Verma, and S. Jain, "Effect of natural fibers surface treatment and their reinforcement in thermo-plastic polymer composites: a review," *Current Organic Synthesis*, vol. 14, no. 2, pp. 186-199, 2017.
- [20] R. Ahmad, R. Hamid, and S. A. Osman, "Physical and chemical modifications of plant fibres for reinforcement in cementitious composites. advances in civil engineering," *Advances in Civil Engineering*, vol. 2019, 2019
- [21] S. R. Ferreira, F. A. Silva, P. R. L. Lima, and R. D. Toledo Filho, "Effect of hornification on the structure, tensile behavior and fiber matrix bond of sisal, jute and curauá fiber cement based composite system," *Construction and Building Materials*, vol. 139, pp. 551-561, 2017.

- [22] S. R. Ferreira, F. A. Silva, P. R. L. Lima, and R. D. Toledo Filho, "Effect of fiber treatments on the sisal fiber properties and fiber–matrix bond in cement based systems," *Construction and Building Materials*, vol. 101, pp. 730-740, 2015.
- [23] S. Jose, S. Thomas, K. P. Jibin, K. S. Sisanth, V. Kadam, and D. B. Shakyawar, "Surface modification of wool fabric using sodium liginosulfonate and subsequent improvement in the interfacial adhesion of natural rubber latex in the wool/rubber composites," *Industrial Crops & Products*, vol. 177, p. 114489, 2022.
- [24] F. Oliveira, C. G. Silva, L. A. Ramos, and E. Frollini, "Phenolic and liginosulfonate-based matrices reinforced with untreated and liginosulfonate-treated sisal fibers," *Industrial Crops & Products*, vol. 96, pp. 30-41, 2017.
- [25] S. L. Gualberto, L. A. C. Motta, and D. Pasquini. "Treatment of sisal fibers with liginosulphonate to improve the properties of fiber cement composites" (in Portuguese), *Revista Virtual de Química*, vol. 13, no. 6, pp. 1257-1267, 2021.
- [26] J. Ruwoldt, "A critical review of the physicochemical properties of liginosulfonates: chemical structure and behavior in aqueous solution, at surfaces and interfaces. Surfaces," *Surfaces*, vol. 3, pp. 622-648, 2020.
- [27] S. Park, J. O. Baker, M. E. Himmel, P. A. Parilla, and D. K. Johnson, "Cellulose crystallinity index: Measurement techniques and their impact on interpreting cellulase performance," *Biotechnology for Biofuels*, vol. 3, pp. 10-19, 2010.
- [28] L. Segal, J. J. Creely, A. E. Martin Jr., and C. M. Conrad, "An empirical method for estimating the degree of crystallinity of native cellulose using the X-Ray diffractometer," *Textile Research Journal*, vol. 29, pp. 786-794, 1962.
- [29] Standard guide for forensic analysis of fibers by infrared spectroscopy, ASTM E2224-19, ASTM International, West Conshohocken, PA, 2019.
- [30] Standard test method for thermal stability by thermogravimetry, ASTM E2550-21, ASTM International, West Conshohocken, PA, 2021.
- [31] Standard test method for tensile strength and Young's modulus of Fibers, ASTM C1557-20, ASTM International, West Conshohocken, PA, 2020.
- [32] P. D. T. O'Connor, and A. Kleyner, *Practical reliability engineering*, West Sussex: John Wiley & Sons, 2012.
- [33] F. Nindiyasari, E. Griesshaber, T. Zimmermann, A. P. Manian, C. Randow, R. Zehbe, L. Fernandez-Diaz, A. Ziegler, C. Fleck, and W. W. Schmahl, "Characterization and mechanical properties investigation of the cellulose/gypsum composite," *Journal of Composite Materials*, vol. 50, no. 5, pp. 657-672, 2015.
- [34] S. Kim, C. Silva, A. Zille, C. Lopez, D. V. Evtuguin, and A. Cavaco-Paulo, "Characterisation of enzymatically oxidized liginosulfonates and their application on lignocellulosic fabrics," *Polymer International*, vol. 58, pp. 863-868, 2009.
- [35] V. S. Sreenivasan, S. Somasundaram, D. Ravindran, V. Manikandan, and R. Narayanasamy, "Microstructural, physicochemical and mechanical characterisation of *Sansevieria cylindrica* fibres – An exploratory investigation," *Materials and Design*, vol. 32, pp. 453-461, 2011.
- [36] S. G. Jebadurai, R. Edwin Raj, V. S. Sreenivasan, and J. S. Binoj, "Comprehensive characterization of natural cellulosic fiber from *Coccinia grandis* stem," *Carbohydrate Polymers*, vol. 207, pp. 675-683, 2019.
- [37] N. V. V. Aguiar, R. M. Vieira, A. P. Matos, and M. R. Forim, "Extraction and characterization of lignin from corn straw (*Zea mays L.*)," (in Portuguese), *Revista Virtual de Química*, vol. 12, no. 6, pp. 1441-1452, 2020.
- [38] S. N. Monteiro, F. P. D. Lopes, A. P. Barbosa, A. B. Bevitori, I. L. A. Silva, and L. L. Costa, "Natural lignocellulosic fibers as Engineering Materials – An Overview," *Metallurgical and Materials Transactions A*, vol. 42A, pp. 2963-2974, 2011.